Model Predictive Control of An Embedded Enhanced-Boost Z-Source Inverter

Yuan, Jing; Yang, Yongheng; Liu, Ping; Blaabjerg, Frede

Published in:
Proceedings of the 19th Workshop on Control and Modeling for Power Electronics, COMPEL 2018

DOI (link to publication from Publisher):
10.1109/COMPEL.2018.8459954

Publication date:
2018

Document Version
Accepted author manuscript, peer reviewed version

Model Predictive Control of An Embedded Enhanced-Boost Z-Source Inverter

Jing Yuan[1], Yongheng Yang[1], Ping Liu[2], Frede Blaabjerg[1]

[1]*Department of Energy Technology, Aalborg University, Denmark*

[2]*College of Electrical and Information Engineering, Hunan University, China*

Email: yua@et.aau.dk, yoy@et.aau.dk, pingliu@hnu.edu.cn, fbl@et.aau.dk

***Abstract*—This paper proposes a model predictive control strategy for an Embedded Enhanced-Boost Z-Source Inverter (EEB-ZSI). Due to many passive components and non-linear power devices in the EEB-ZSI, the closed-loop control with proportional integral (PI) controllers based on the small signal modelling is impractical. However, the proposed model predictive control strategy can achieve closed-loop control in terms of accuracy and dynamics, where the complicated modeling is not necessary. In the proposed method, only two capacitor voltages and two inductor currents are considered due to the symmetry. Simulation results are provided to validate the performance of the proposed control strategy.**

Keywords—model predictive control, impedance source converter

I. INTRODUCTION

Conventional voltage source inverters (VSIs) are widely used in industry, e.g., in electric vehicles and grid-connected renewable energy systems [1]. In such applications, a dc-dc boost converter is added to obtain a desired dc-link voltage (e.g., 400 V for single-phase systems and 650 V for three-phase systems), which, however, increases the system cost and lowers the efficiency. Impedance source converters, e.g., the Z-source inverter (ZSI) [2] and the quasi Z-source (qZSI) inverter [3], as single-stage systems, address those issues to a great extent. Hence, many attempts have been made to improve the performance of impedance source converters (e.g., ZSI and qZSI) through topological innovations and/or advanced control [4]-[6]. Notably, one important feature of impedance source converters is the capability to achieve high conversion ratios (boost ratios), which are dependent of the passive components (i.e., impedance networks).

As such, in order to increase the boost capability, more passive components are added to the classic ZSI or quasi-ZSI (qZSI). The switched-impedance network based converter is an example [4], as shown in Fig. 1, to achieve an even higher boost factor compared with the traditional ZSI/qZSI. In addition, the switched inductor/capacitor ZSI (SI-ZSI) can provide continuous input current and reduced voltage stress of the capacitor. However, it is very difficult to control the dc-link voltage in a closed-loop control system due to the high-order characteristics (i.e., many passive components).

In the literature, most of the prior-art closed-loop control methods focus on the conventional ZSI or qZSI, using proportional integral (PI) controllers [7]-[10]. Yet, it is very difficult to control the modified ZSIs with many passive components, e.g., the Embedded Enhanced-Boost Z-source Inverter (EEB-ZSI) shown in Fig. 2. The Model Predictive Control (MPC) is a powerful control method avoiding the small signal modelling and the modulation, and thus it may be a promising solution to high-order ZSIs in terms of control accuracy, dynamics, and simplicity [10]. The MPC has been successfully applied to the conventional ZSI [11] and qZSI to control the load current, inductor current, and capacitor voltage [13]-[15], which further demonstrates its superior performance. As there are more state variables in high-order switched-impedance ZSIs, MPC overcomes the limitation of multivariable systems.

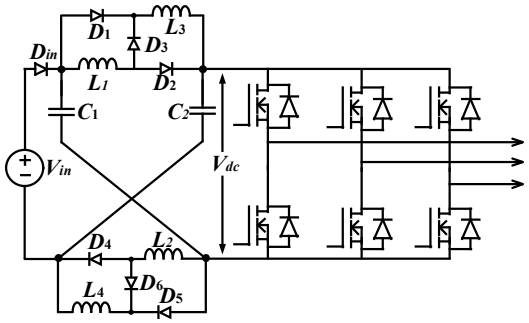

Fig. 1. Three-phase switched-inductor Z-source inverter (SI-ZSI) [4].

Inspired by the above, this paper introduces a model predictive current control method for the EEB-ZSI. The proposed MPC strategy can control the inductor current and capacitor voltage to obtain a desired load current and stabilize the system. In § II, the operation principle of the EEB-ZSI are presented. A detailed MPC current control strategy is illustrated in § III. Simulation results are provided in § IV, which verify the high dynamic performance of the proposed model predictive current control strategy. Finally, the conclusion are demonstrated.

II. OPERATION PRINCIPLE OF THE EEB-ZSI

The EEB-ZSI has the shoot-through state and non-shoot-through state. It is assumed that all capacitors (and inductors) in the EEB-ZSI are identical. Moreover, the dc sources in the Z-source networks, as shown in Fig. 2, are the same. Based on the symmetrical topology, the following hold:

$$V_{C1} = V_{C2} \tag{1}$$

$$V_{C3} = V_{C4} \tag{2}$$

$$i_{L1} = i_{L2} \tag{3}$$

$$i_{L3} = i_{L4} \tag{4}$$

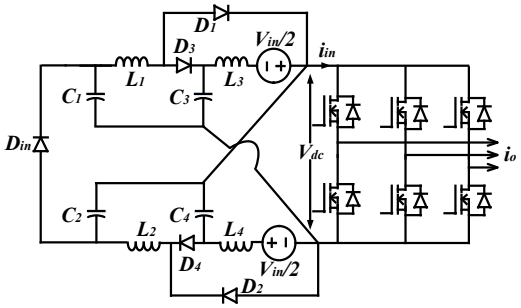

Fig. 2. Embedded enhanced-boost Z-source inverter.

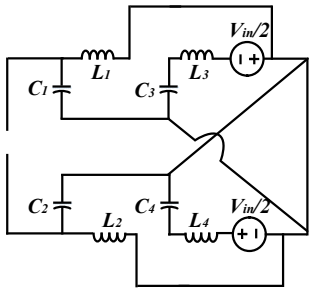

Fig. 3. Shoot-through state of the EEB-ZSI.

in which V_{C1}, V_{C2}, V_{C3}, and V_{C4} are the corresponding voltage across the capacitor C_1, C_2, C_3, and C_4, i_{L1} , i_{L2}, i_{L3} , and i_{L4} are the inductor currents. For simplicity, only i_{L1}, i_{L3} and V_{C1}, V_{C3} are considered in the following analysis.

In *Shoot-Through State*, D_1 and D_2 are ON with D_3, D_4, and D_{in} being reverse-biased. Additionally, L_1 and L_2 are in parallel with C_1 and C_2, respectively, which are shown in Fig. 3. This leads to

$$\frac{dV_{C1}}{dt} = -\frac{1}{C} i_{L1} \tag{5}$$

$$\frac{dV_{C3}}{dt} = -\frac{1}{C} i_{L3} \tag{6}$$

$$\frac{di_{L1}}{dt} = \frac{1}{L} V_{C1} \tag{7}$$

$$\frac{di_{L3}}{dt} = \frac{1}{L} V_{C3} + \frac{1}{2L} V_{in} \tag{8}$$

In *Non-Shoot-Through State*, D_3, D_4, and D_{in} are ON, and D_1 and D_2 are OFF as shown in Fig. 4. Thus, the capacitor voltages and inductor currents are expressed as

$$\frac{dV_{C1}}{dt} = \frac{1}{C}\left(-i_{L1} + i_{L3} + i_{L4} - i_{in}\right) \tag{9}$$

$$\frac{dV_{C3}}{dt} = \frac{1}{C}\left(i_{L1} - i_{L3}\right) \tag{10}$$

$$\frac{di_{L1}}{dt} = \frac{1}{L}\left(V_{C1} - V_{C3}\right) \tag{11}$$

$$\frac{di_{L3}}{dt} = \frac{1}{L}\left(-V_{C1} - V_{C2} + V_{C3}\right) + \frac{1}{2L} V_{in} \tag{12}$$

Additionally, according to the volt-second balance principle and the Kirchhoff's law, we have

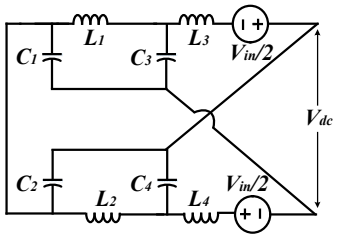

Fig. 4. Non-shoot-through state of the ZSI.

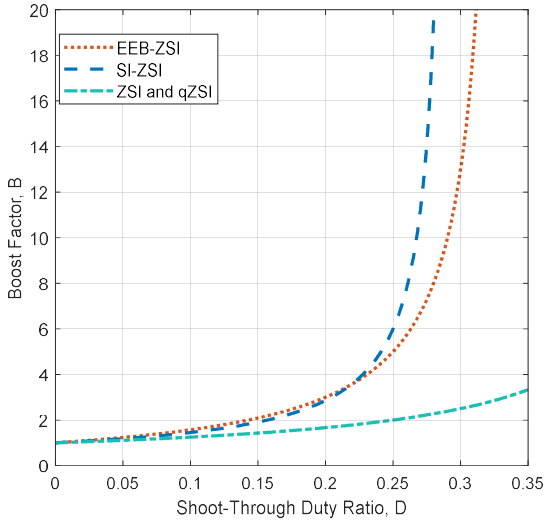

Fig. 5. Boost factor comparison of three Z-source inverters (i.e., the ZSI/qZSI, SI-ZSI, and EEB-ZSI).

$$V_{C1} = (1-D) V_{C3} \tag{13}$$

$$i_{L3} = (1-D) i_{L1} \tag{14}$$

where D is the duty ratio. The capacitor voltage V_{C3} and the peak dc-link voltage $\hat{V}_{dc}$ can then be expressed as

$$V_{C3} = \frac{0.5}{2D^2 - 4D + 1} V_{in} \tag{15}$$

$$\hat{V}_{dc} = \frac{1-D}{2D^2 - 4D + 1} V_{in} = B \cdot V_{in} \tag{16}$$

where

$$B = \frac{1-D}{2D^2 - 4D + 1} \tag{17}$$

is the boost factor. Fig. 5 shows the relationship between the shoot-through duty ratio and the boost factor among ZSI/qZSI, SI-ZSI, and EEB-ZSI topologies. It is clear that the boost factor of the EEB-ZSI is higher than the ZSI/qZSI and SI-ZSI with the same shoot-through value.

According to (15) and (16), the average dc-link voltage, which is used to calculate the voltage space vector, can be obtained as

$$V_{average-dc} = \hat{V}_{dc}(1-D) = \frac{2V_{C1}^2}{V_{C3}} \tag{18}$$

where $V_{average-dc}$ is the average dc-link voltage.

III. Model Predictive Current Control Strategy for the EEB-ZSI

A. Modeling of the EEB-ZSI

The EEB-ZSI switching states are the same as the traditional ZSI or qZSI – 6 active states, 2 null states, and 7 shoot-through states [13]. When the null states and all shoot-through states occur, the output voltage vectors are zero. The relationship between the output voltage space vectors and the switching states is shown in Table I. The proper voltage vector for the system is chosen by applying the model predictive current control strategy. The output voltages in Fig. 6 can be expressed using space vector as:

$$V_i = \frac{2}{3}\left(v_{aN} + a v_{bN} + a^2 v_{cN}\right) \qquad a = -\frac{1}{2} + j\frac{\sqrt{3}}{2} \tag{19}$$

where v_{aN},v_{bN} and v_{cN} are the phase voltage as shown in Fig. 6.

Assuming that the load of the inverter consists of a resistor R_{load} and an inductor L_{load} per phase, thus

$$L_{load}\frac{di_o}{dt} = V_i - i_o R_{load} \tag{20}$$

where i_o is the output three-phase current. With the Euler method, (19) can be discretized as

$$i_o\left(t+T_s\right)_{(\alpha,\beta)} = \frac{L_{load} i_o\left(t\right)_{(\alpha,\beta)} + T_s \times V_i\left(t+T_s\right)}{L_{load} + R_{load} T_s} \tag{21}$$

in which T_s is the sampling period and the point t is the current time when the input comes into the controller. The grid current is converted from the *abc*-natural reference frame to the *αβ*-stationary reference frame (three variables to two variables), which simplifies the control implementation.

B. Predictive model for the EEB-ZSI

In order to implement the MPC, i_{L1}, i_{L3} and V_{C1}, V_{C3} can be selected as control variables. The discrete equations can be derived from the shoot-through states and the non-shoot-through states based on equations (5)-(12). More specifically, In the shoot-through state, (5)-(8) can be discretized as

$$i_{L1}\left(t+T_s\right) = i_{L1}\left(t\right) + \left(\frac{T_s}{L}\right)\times\left(V_{C1}\left(t+T_s\right)\right) \tag{22}$$

$$i_{L3}\left(t+T_s\right) = i_{L1}\left(t\right) + \frac{\left(T_s\right)}{L}\times V_{C3}\left(t+T_s\right) + \frac{T_s}{2L}\times V_{in} \tag{23}$$

$$V_{C1}\left(t+T_s\right) = V_{C1}\left(t\right) - \left(\frac{T_s}{C}\right)\times i_{L1}\left(t+T_s\right) \tag{24}$$

$$V_{C3}\left(t+T_s\right) = V_{C3}\left(t\right) - \frac{T_s}{C}\times i_{L3}\left(t+T_s\right) \tag{25}$$

In the non-shoot-through state, the discrete equations are

TABLE I.
RELATIONSHIP BETWEEN THE SWITCHING STATES AND THE OUTPUT VOLTAGE VECTORS.

S_a	S_b	S_c	Voltage Vector V_i
1	0	0	$V_1 = \frac{2}{3}V_{dc}$
1	1	0	$V_2 = \frac{1}{3}V_{dc} + j\frac{\sqrt{3}}{3}V_{dc}$
0	1	0	$V_3 = -\frac{1}{3}V_{dc} + j\frac{\sqrt{3}}{3}V_{dc}$
0	1	1	$V_4 = -\frac{2}{3}V_{dc}$
0	0	1	$V_5 = -\frac{1}{3}V_{dc} - j\frac{\sqrt{3}}{3}V_{dc}$
1	0	1	$V_6 = \frac{1}{3}V_{dc} - j\frac{\sqrt{3}}{3}V_{dc}$
Null and all shoot-through states			$V_7 = 0$

$$i_{L1}\left(t+T_s\right) = i_{L1}\left(t\right) + \left(\frac{T_s}{L}\right)\times\left(V_{C1}\left(t+T_s\right) - V_{C3}\left(t+T_s\right)\right) \tag{26}$$

$$i_{L3}\left(t+T_s\right) = i_{L1}\left(t\right) - \frac{T_s}{L}\left(2V_{C1}\left(t+T_s\right) - V_{C3}\left(t+T_s\right) - \frac{V_{in}}{2}\right) \tag{27}$$

$$V_{C1}\left(t+T_s\right) = V_{C1}\left(t\right) + \left(\frac{T_s}{C}\right)\times \left(-i_{L1}\left(t+T_s\right) + 2i_{L3}\left(t+T_s\right) - i_{in}\left(t+T_s\right)\right) \tag{28}$$

$$V_{C3}\left(t+T_s\right) = V_{C3}\left(t\right) + \frac{T_s}{C}\times\left(i_{L1}\left(t+T_s\right) - i_{L3}\left(t+T_s\right)\right) \tag{29}$$

C. Proposed MPC for the EEB-ZSI

The entire MPC process consists of three steps. Firstly, the control variables such as inductor currents and capacitor voltages are measured. The second step is to predict the future states of the control variables according to the measurements. Finally, the best switching states can be obtained by minimizing a predefined cost function. The entire control system is shown in Fig. 6.

In addition to the system model, another important aspect of the MPC is how to design a proper cost function, which is used to optimize the output voltage vectors. The proposed cost function in this paper includes the output load current (i_o), two capacitor voltages (V_{C1}, V_{C3}), and two inductor currents (i_{L1}, i_{L3}). The cost function of the load currents (i.e., the *αβ*-axis currents) is defined as

$$g_{io} = \left|i_{o\alpha}{}^{*} - i_{o\alpha}\left(t+T_s\right)\right| + \left|i_{o\beta}{}^{*} - i_{o\beta}\left(t+T_s\right)\right| \tag{30}$$

in which $i^*_{o\alpha}$ and $i^*_{o\beta}$ represent the *α*- and *β*-component of the reference current, $i_{o\alpha}$ $(t+T_s)$ and $i_{o\beta}$ $(t+T_s)$ are the *α*- and *β*-component of the predicted grid current. The inductor current cost functions g_{iL1} and g_{iL3} are expressed as

$$g_{iL1} = \left|i_{L1}{}^{*} - i_{L1}\left(t+T_s\right)\right| \tag{31}$$

$$g_{iL3} = \left|i_{L3}{}^{*} - i_{L3}\left(t+T_s\right)\right| \tag{32}$$

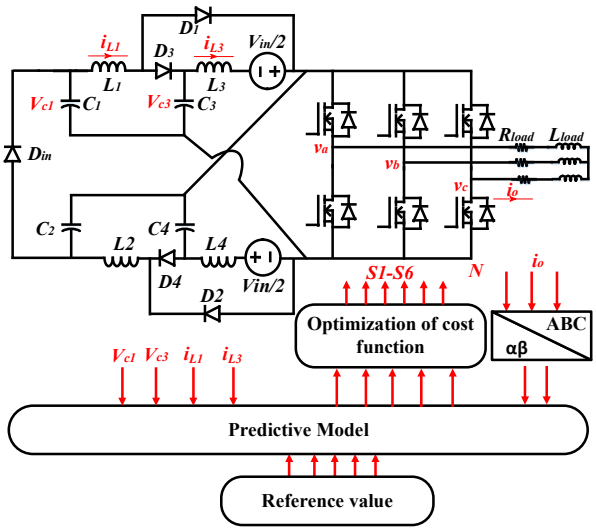

Fig. 6. Control diagram of the EEB-ZSI using the MPC method.

with i_{L1}^{*}, i_{L3}^{*}, and $i_{L1}(t+T_s)$, $i_{L3}(t+T_s)$ being the inductor current references and the predicted inductor currents, correspondingly. The capacitor voltage cost functions g_{VC1} and g_{VC3} are given as

$$g_{VC1} = \left| V_{C1}^{*} - V_{C1}(t+T_s) \right| \tag{33}$$

$$g_{VC3} = \left| V_{C3}^{*} - V_{C3}(t+T_s) \right| \tag{34}$$

where V_{C1}^{*}, V_{C3}^{*}, and $V_{C1}(t+T_s)$, $V_{C3}(t+T_s)$ and represent the capacitor voltage references and the corresponding predicted variables.

As a result, the entire cost function g can be expressed with five weighting factors as

$$g = \lambda_1 g_{io} + \lambda_2 g_{iL1} + \lambda_3 g_{iL3} + \lambda_4 g_{VC1} + \lambda_5 g_{VC3} \tag{35}$$

in which λ_i (i = 1, 2, 3, 4, 5) denotes the weighting factor for the output load current i_o, the inductor currents of L_1 and L_3, and the capacitor voltages of C_1 and C_3. In this paper, the values of the weighting factors are tuned with the trial and error method.

The flowchart of the MPC for the EEB-ZSI is shown in Fig. 7. As aforementioned, the first step is to measure the five control variables. Then, the predicted load current is calculated according to (20). By determining that if it is the non-shoot through state or the shoot through state, the corresponding control variables are calculated following (22)-(25) or (26)-(29). The algorithm can obtain the optimal switching state by minimizing the cost function. Finally, the resultant optimal switching states are used to drive the power devices of the inverter.

IV. Simulation Results

To evaluate the performance of the proposed MPC strategy, a MATLAB/Simulink model with the MPC strategy is built up. The parameters of the system are shown in Table II. The MPC controller can be implemented easily in MATLAB as C-function files. In terms of the choice for the weighting factors, they are obtained by the trial and error method and the weighting factors λ_i (i = 1, 2, 3, 4, 5) in simulations are selected as 1, 1, 1, 5, 5.

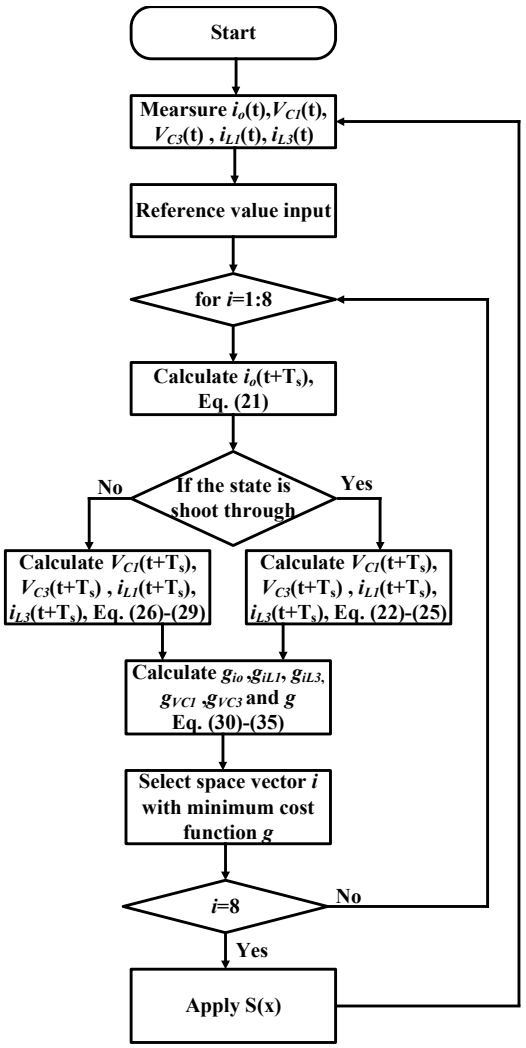

Fig. 7. Flow chart of the proposed MPC for the EEB-ZSI.

Fig. 8 shows that the three-phase load currents are sinusoidal and the peak current in the beginning is 7 A. At t = 1.5 s, there is a step change for the load current reference value. It is observed that the output load current changes from 7 A to 5 A with a good tracking capability. More importantly, the dynamics of the control are fast.

Moreover, the inductor current reference is related to the input power and input dc voltage. When the load current reference changes, the inductor current references have the same variation tendency with a constant input dc voltage. The simulation results of the inductor current are shown in Fig. 9. The reference inductor currents i_{L1}, i_{L2} and i_{L3}, i_{L4} are changed from 32.5 A to 26 A and from 24.4 A to 19.5 A, respectively. The inductor currents are continuous, and they can also follow the reference inductor currents after a short transient period, as it is shown in Fig. 9. In order to achieve a dc-link voltage boosted from 100 V to 600 V, the references of V_{C1} and V_{C2} are 300 V, while the references for V_{C3} and V_{C4} are 400 V based on the equations (13)-(16). From the simulation results in Figs. 10 and 11, it can be seen that the dc-link voltage is boosted from 100 V to 600 V and capacitor voltages remain constant at 300 V and 400 V, as expected.

TABLE II.
SIMULATION PARAMETERS OF THE EEB-ZSI SYSTEM.

Parameter	Value
DC input voltage	100 V
EEB-ZSI inductance	700 μH
EEB-ZSI capacitor	500 μF
Load inductance	5 mH
Load resistance	30 Ω
Sample time	30 μs

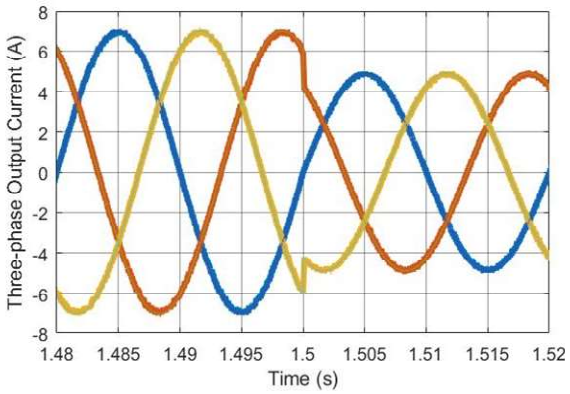

Fig. 8. Simulation results (three-phase output load currents) of the EEB-ZSI with the MPC algorithm under a load step change.

Moreover, the capacitor voltages have slight variations in the transient periods. Nonetheless, the above simulation results have demonstrated that the MPC algorithm can effectively control the high-order impedance source converters (i.e., the EEB-ZSI) with relatively high accuracy and fast dynamics. It should be pointed out that the important aspect for the MPC is to properly design the corresponding weighting factors.

V. CONCLUSION

In this paper, a model predictive current control method for an Embedded Enhanced-Boost Z-source Inverter was proposed. The proposed MPC was implemented considering the output current, the capacitor voltage, and the inductor current. Considering that the traditional PI controller is suitable for low-order systems, the proposed MPC can overcome the limitation of high-order multivariable systems that are difficult to control using PI controllers. Simulation results have demonstrated that the proposed strategy has a good dynamic performance while maintaining a stable dc-link voltage. Hence, the proposed MPC strategy can be a promising solution to the Embedded Enhanced-Boost impedance source inverter.

ACKNOWLEDGMENT

This work was conducted at Center of Reliable Power Electronics (CORPE) at Aalborg University, Denmark, and was supported in part by China Postdoctoral Science Foundation under Grant 2016M602406.

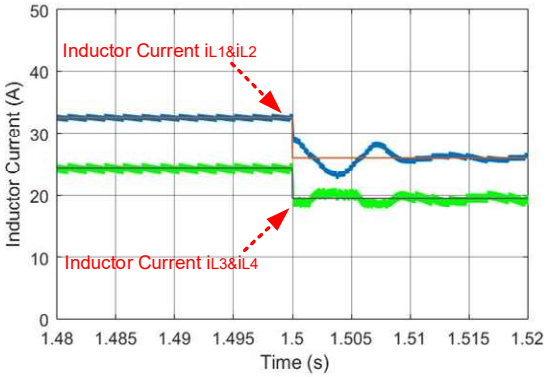

Fig. 9. Simulation results (inductor currents) of the EEB-ZSI, where the inductor current references are changed.

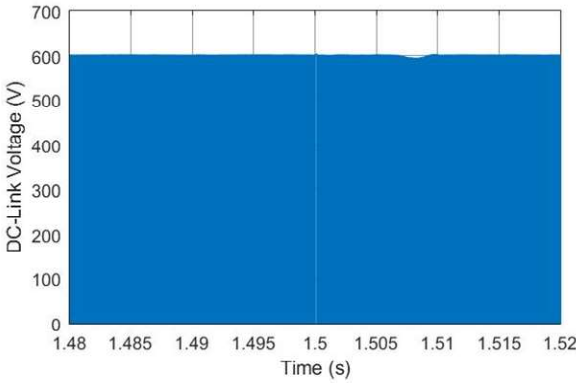

Fig. 10. Simulation results (the DC-link voltage) of the EEB-ZSI.

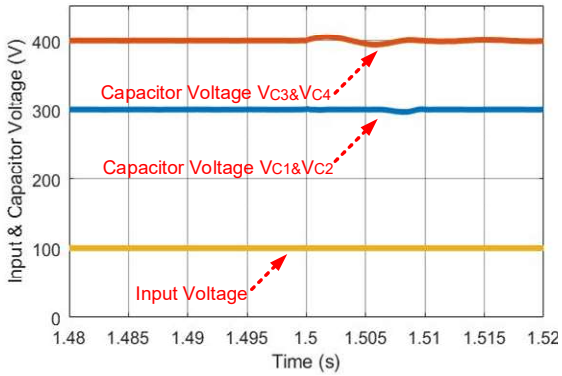

Fig. 11. Simulation results (the input voltage and capacitor voltages) of the EEB-ZSI under a step change of the inductor current references.

REFERENCES

[1] Y. P. Siwakoti, F. Z. Peng, F. Blaabjerg, P. C. Loh, and G. E. Town, "Impedance Source network for electric power conversion—Part I: A topological review," in *IEEE Trans. Power Electron.*, vol. 30, no. 2, pp. 699-716, Feb. 2015.

[2] F. Z. Peng, "Z-source inverter," in *IEEE Trans. Ind. Appl.*, vol. 39, no. 2, pp. 504-510, Mar. 2003

[3] J. Anderson and F. Z. Peng, "Four quasi-Z-Source inverters," in *Proc. of 2008 IEEE Power Electronics Specialists Conference*, Rhodes, 2008, pp. 2743-2749.

[4] M. Zhu, K. Yu, and F. L. Luo, "Switched inductor Z-source inverter," in *IEEE Trans. Power Electron.*, vol. 25, no. 8, pp. 2150-2158, Aug. 2010.

[5] M.-K. Nguyen, Y.-C. Lim, and J.-H. Choi, "Two switched-inductor quasi-Z-source inverters," in *IET Power Electron.*, vol. 5, no. 7, pp. 1017-1025, 2012.

[6] H. Fathi and H. Madadi, "Enhanced-Boost Z-Source Inverters With Switched Z-Impedance," in *IEEE Trans. Ind. Electron*, vol. 63, no. 2, pp. 691-703, Feb. 2016.

[7] X. Ding, Z. Qian, S. Yang, B. Cui, and F. Peng, "A PID Control Strategy for DC-link Boost Voltage in Z-source Inverter," in *Proc. of IEEE Applied Power Electronics Conference and Exposition*, Anaheim, CA, USA, 2007, pp. 1145-1148.

[8] F. Guo, L. Fu, C. H. Lin, C. Li, W. Choi, and J. Wang, "Development of an 85-kW Bidirectional Quasi-Z-Source Inverter With DC-Link Feed-Forward Compensation for Electric Vehicle Applications," in *IEEE Trans. Power Electron.*, vol. 28, no. 12, pp. 5477-5488, Dec. 2013.

[9] Y. Liu, B. Ge, H. Abu-Rub, and F. Z. Peng, "Control System Design of Battery-Assisted Quasi-Z-Source Inverter for Grid-Tie Photovoltaic Power Generation," in *IEEE Trans. Sustain. Energy*, vol. 4, no. 4, pp. 994-1001, Oct. 2013.

[10] C. J. Gajanayake, D. M. Vilathgamuwa and P. C. Loh, "Development of a Comprehensive Model and a Multiloop Controller for Z-Source Inverter DG Systems," in *IEEE Trans. Ind. Electron.*, vol. 54, no. 4, pp. 2352-2359, Aug. 2007.

[11] W. Mo, P. C. Loh and F. Blaabjerg, "Model predictive control for Z-source power converter," in *Proc. of 8th International Conference on Power Electronics - ECCE Asia*, Jeju, 2011, pp. 3022-3028.

[12] Y. P. Siwakoti, F. Z. Peng, F. Blaabjerg, P. C. Loh, G. E. Town and S. Yang, "Impedance-Source Networks for Electric Power Conversion Part II: Review of Control and Modulation Techniques," in *IEEE Trans. Power Electron.*, vol. 30, no. 4, pp. 1887-1906, April 2015.

[13] M. Mosa, R. S. Balog and H. Abu-Rub, "High-Performance Predictive Control of Quasi-Impedance Source Inverter," in *IEEE Trans. Power Electro.*, vol. 32, no. 4, pp. 3251-3262, April 2017.

[14] A. Ayad, P. Karamanakos and R. Kennel, "Direct model predictive control with an extended prediction horizon for quasi-Z-source inverters," in *Proc. of IECON 2016 - 42nd Annual Conference of the IEEE Industrial Electronics Society*, Florence, 2016, pp. 3348-3353.

[15] A. Bakeer, M. A. Ismeil and M. Orabi, "A Powerful Finite Control Set-Model Predictive Control Algorithm for Quasi Z-Source Inverter," in *IEEE Trans. Ind. Informat.*, vol. 12, no. 4, pp. 1371-1379, Aug. 2016.